IFSR-1011

Nonlinear physics of laser-irradiated micro-clusters

Boris N. Breizman, Alexey V. Arefiev, and Mykhailo V. Fomyts'kyi

Institute for Fusion Studies, The University of Texas, Austin, Texas 78712

(Dated: January 11, 2005)

Abstract

A nonlinear theory has been developed to describe electron response and ion acceleration in dense clusters that are smaller in size than the laser wavelength. This work is motivated by high-intensity laser-cluster interaction experiments. The theory reveals that the breakdown of quasi-neutrality affects the cluster dynamics in a dramatic way: the laser can create a positively charged ion shell that expands due to its own space charge much faster than the central part of the cluster. The developed theory also shows a trend for the electron population to have a two-component distribution function: a cold core that responds to the laser field coherently and a hot halo that undergoes stochastic heating. The hot electrons expand together with the equal number of ions that are accelerated to supersonic velocities in a double layer at the cluster edge. This mechanism produces fast ions with energies much greater than the ponderomotive potential and it suggests that larger deuterium clusters can significantly enhance the neutron yield in future experiments.

I. INTRODUCTION

Intensities of present-day short-pulse lasers routinely exceed the ionization threshold for individual atoms by several orders of magnitude [1, 2]. At these intensities, any gas target virtually instantly turns into plasma under the laser beam. In many experiments, the target is a cold supersonic jet that contains both gas and condensed substance in the form of small-size clusters. The clusters are typically smaller than the laser wavelength. Their concentration and size can be controlled by varying sort of gas and thermodynamic parameters. Similarly to the ambient gas, the clusters easily become plasma under an intense laser beam. However, on a short time-scale they usually do not expand sufficiently to loose their identity. As a result, the laser creates plasma with extremely high and narrow local peaks in the ion density. These peaks can comprise a significant fraction of all plasma ions. The presence of clusters introduces remarkable new phenomena that would never occur in homogeneous gaseous plasma. Both single-cluster behavior and average response of many clusters exhibit interesting features, which makes laser-cluster interaction a very attractive research topic. Two experimental findings are of particular interest: fusion reactions from exploding deuterium clusters [1, 3, 4] and radiation at harmonics of the laser frequency [5, 6]. In this paper, we will focus on physics mechanisms that are relevant to fusion events in exploding clusters. Mechanisms for harmonic generation in individual clusters have been identified in Refs. [7–9], but more work still needs to be done to assess coherent manifestations of these mechanisms under conditions when phase matching effects are involved.

A common explanation for cluster explosion is that the laser field quickly pulls all the electrons out of the cluster, and the un-neutralized ions then fly apart, pushed by the Coulomb forces. It is noteworthy that this scenario implies strong deviation from quasi-neutrality, which appears to be an important aspect of the laser-cluster interaction. From the theoretical standpoint, this indicates that the electron dynamics is fundamentally nonlinear (and hardly tractable analytically) even in the less extreme case when only a fraction of electrons leaves the cluster. Still, progress can be made in the analysis, with the use of the relevant simplifying assumptions that clusters are much smaller than the laser wavelength and that the electron plasma frequency inside the cluster is considerably greater than the laser frequency. This analysis reveals two different populations of electrons. One population is confined within the cluster and it establishes a relatively cold core that responds coherently

to the laser field. The other population either leaves the cluster for good or undergoes stochastic heating as the electrons return and cross the cluster boundary in their bounce motion. The two-component structure of the electron distribution function affects the whole dynamics of cluster expansion on the ion time scale, making it significantly different from what would occur in the case of thermalized Maxwellian electrons. In particular, considerable changes occur in the energy spectrum of the fast ions and in their angular distribution. As a result, the neutron yield from exploding deuterium clusters should also be affected strongly.

Our objective here is to outline and review physics mechanisms and qualitative trends rather than interpret the experimental data quantitatively and conclusively. The latter would generally require an extensive numerical modelling of the anticipated dominant physics mechanism for specific experimental conditions, and subsequent additional measurements to validate the results. The qualitative estimates and simplified problems discussed in this paper may serve as test cases for subsequent more realistic numerical modelling and they also point to physics-based simplifications that can be used to facilitate numerical efforts.

This paper is organized as follows. In Sec. II, we discuss the electron dynamics for a given ion configuration under the assumption that the cluster ions are immobile. In Sec. III, we describe the ion dynamics for small, medium, and large clusters. In Sec. IV, we explain the origins of the ion anisotropy. In Sec. V, we give a rigorous solution for the double layer and the resulting quasi-neutral plasma flow in the case of a large cluster. Section VI consists of concluding remarks.

II. ELECTRON DYNAMICS

In this section, we describe the electron dynamics for a given ion configuration, assuming that the cluster ions are immobile. In a typical experiment, the cluster radius (R_0) is much smaller than the laser wavelength. As a result, the electric field of the laser can be treated as a time-dependent spatially uniform external field, when considering a single cluster.

We start by considering a uniform spherical cluster, with ion density n_0, in a uniform static electric field E_0. The field extracts electrons from the cluster, making the cluster positively charged. If all the electrons are extracted, the cluster becomes a uniform ion sphere with the total charge $(4/3)\pi R_0^3 n_0|e|$. In this case, the electric field created by the

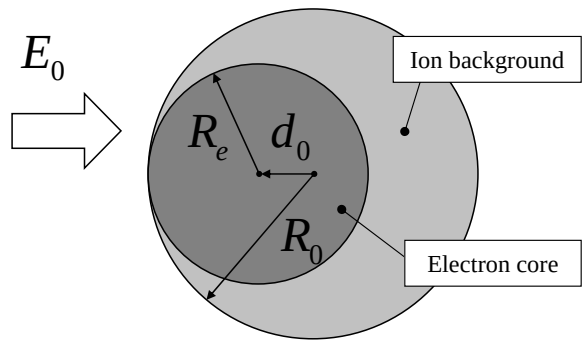

FIG. 1: Equilibrium configuration of the electrons confined in a uniform spherical cluster in the presence of a static electric field [10]. The outer circle marks the edge of the ion background and the inner circle marks the boundary of the confined electron population. The light-grey area corresponds to the uncompensated ion space-charge.

cluster increases from zero at the center to

$$E_{\max} = \frac{4}{3}\pi R_0 n_0 |e| \tag{1}$$

at the cluster edge and then decreases radially outside the cluster. The external field can extract all the electrons from the cluster only if $E_0 > E_{\max}$.

If $E_0 < E_{\max}$, then some electrons remain inside the cluster, forming a cold spherical electron core with the electron density equal to n_0 [10]. The radius of the core is $R_e = R_0 - d_0$ and the core is offset by d_0 from the center of the cluster in the direction opposite to the direction of the electric field (see Fig. 1), where

$$d_0 \equiv 3\frac{|e|E_0}{m_e \omega_{p0}^2}, \tag{2}$$

with $\omega_{p0}^2 \equiv 4\pi n_0 e^2/m_e$. The self-consistent field of the cluster cancels the external field inside the electron core, so that the cold core electrons are in an equilibrium. If the core displacement is relatively small ($d_0 \ll R_0$), we find that the total number of the extracted electrons is

$$N_{ext} \approx 4\pi n_0 R_0^2 d_0, \tag{3}$$

whereas, in general, we have $N_{ext} = \frac{4}{3}\pi n_0 [R_0^3 - (R_0 - d_0)^3]$. Finally, it must be pointed out that this configuration is assumed to be achieved by increasing the electric field from zero to E_0 on a time scale much longer than $1/\omega_{p0}$, so that the confined electrons adjust

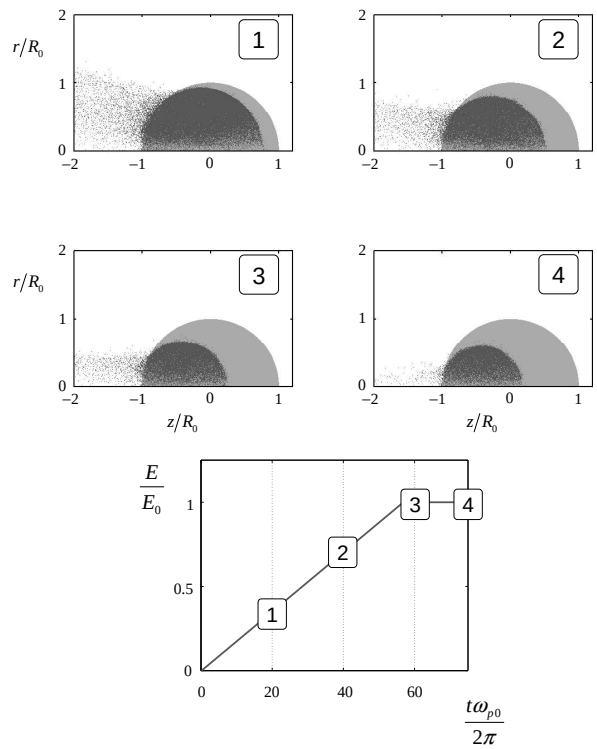

FIG. 2: Particle-in-cell simulation of the electron core formation in a slowly increasing electric field. Monotonically increasing applied electric field (E) extracts electrons (dark-grey) as the core contracts (1-3). The contraction stops when the external field saturates (3-4). The immobile ion background (light-grey) is uniform in this case. The lower plot shows the time dependence of the applied field.

adiabatically to the electric field [10]. We have carried out a particle-in-cell simulation to demonstrate the electron core formation in a slowly increasing electric field. The results of the simulation are shown in Fig. 2.

A similar configuration also exists for a nonuniform cluster of arbitrary shape. We have developed a code that allows us to quickly find an equilibrium configuration of the confined electrons for an arbitrary shaped cluster using the artificial electron boundary dynamics [10]. An example of a calculation for a radially nonuniform axisymmetric spherical cluster is shown in Fig. 3. The equilibrium configuration of the electron core is not spherical in this case and it has such shape that the electrostatic potential inside the electron core is flat.

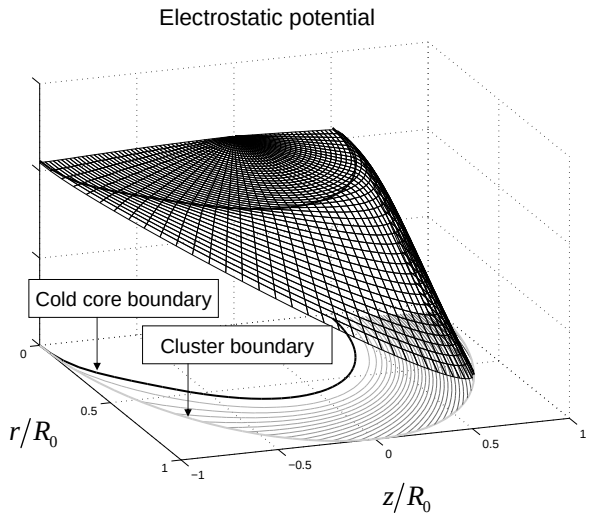

FIG. 3: Equilibrium electrostatic potential inside a spherical cluster with radially nonuniform ion density. The solid black line shows the boundary of the electron core.

Having discussed the case with a static external electric field, we now turn to the case when the external electric field oscillates at the laser frequency. As already stated, the cold core electrons adjust adiabatically to the laser field, i.e. the laser field is effectively static for them. The key difference is in the dynamics of the extracted electrons. The characteristic energy that they gain in the laser field is

$$\varepsilon \approx \frac{m_e}{2}\left(\frac{eE_0}{m_e\omega}\right)^2, \tag{4}$$

where ω is the laser frequency. On the other hand, the characteristic binding energy of the extracted electrons to the cluster can be estimated as

$$U \approx e^2 N_{ext}/R_0. \tag{5}$$

The extracted electrons are not bound to the cluster if $\varepsilon \gg U$, which is equivalent to the condition that the quivering amplitude of a free electron, ξ, is greater than the cluster radius, where

$$\xi \equiv \frac{|e|E_0}{m_e\omega^2}. \tag{6}$$

At $\xi \gg R_0$, the extracted electrons never return to the cluster. Their characteristic energy after the pulse is of the order of U, which is smaller than the characteristic quivering energy ε. This case is similar to the case with a static external electric field, because the laser

frequency ω is sufficiently low. The electron core inside the cluster will move in step with the laser field, so that the core displacement is proportional to the instantaneous value of the field.

In the opposite regime with $\xi \ll R_0$, the extracted electrons are bound to the cluster and they undergo stochastic heating, as described in the next subsection.

In presence of collisions, the oscillating electron core will also be heated. However, the rate of collisional heating is a rapidly decreasing function of the electron temperature. As a result, collisional heating virtually stops at about 1-2 keV [1], whereas stochastic heating of the extracted electrons is able to provide much greater particle energies.

Stochastic heating

Since the characteristic excursion of the extracted electrons is much smaller than the cluster radius ($\xi \ll R_0$), the electron heating problem becomes effectively one dimensional. As the laser field starts to increase, some electrons are pulled out of the cluster in order to maintain zero field inside the cluster. The number of electrons (per unit area of the cluster) that must be pulled out in order to shield the cluster from the laser field is roughly $N_{ext}/4\pi R_0^2 \approx n_0 d_0$ [see Eq. (3)]. As the laser field reverses, the extracted electrons are pushed back into the cluster. The characteristic energy of these (warm) electrons is ε. There is no electric field inside the cluster, so that, after reentering the cluster, the warm electrons continue moving freely with velocity $\sqrt{\varepsilon/m_e}$ through the cluster. During the next period, the laser field produces another generation of warm electrons in exactly the same way. At this stage, the process is similar to the conventional vacuum heating [11, 12].

The situation changes after the time interval

$$\tau \approx \frac{R_0}{\sqrt{\varepsilon/m_e}} \approx \frac{1}{\omega}\frac{R_0}{\xi}, \tag{7}$$

required for a warm electron to cross the cluster. By this time, the warm electrons with the density $n_0 d_0/\xi$ fill the entire cluster and extend into the vacuum beyond the cluster edge. They shield the cluster from the laser field, precluding any further extraction of the cold

electrons from the cluster. We estimate the maximum number of the warm electrons as

$$N_H \approx 4\pi R_0^2 d_0 n_0 \omega \tau \approx N_0 \frac{\omega^2}{\omega_{p0}^2}, \tag{8}$$

where N_0 is the total number of ions in the cluster. N_H is considerably smaller than the number of the cold electrons, because ω is much smaller than ω_{p0}.

At $t < t_0 + \tau$, the characteristic energy of the warm electrons is ε, with t_0 corresponding to the beginning of the laser pulse. At $t > t_0 + \tau$, these electrons heat up, as they gain energy of order ε every time they come out into the vacuum after passing through the cluster [2, 10]:

$$\varepsilon_e \approx m_e \frac{t^2}{R_0^2} \left(\frac{eE_0}{m_e \omega} \right)^4. \tag{9}$$

The stochastic heating is effective as long as the electron transit time through the cluster is large compared to the wave period: $R_0/\sqrt{\varepsilon/m_e} \geq 1/\omega$, so that the transiting electrons have time to go out of phase with the wave. Thus the maximum energy that an electron can gain via the stochastic heating is

$$\max \varepsilon_e \approx \frac{1}{2} m_e R_0^2 \omega^2. \tag{10}$$

It must be pointed out that, in the limit of $\xi \ll R_0$, this energy is much higher than the electron quivering energy in the laser field: $\max \varepsilon_e \approx \varepsilon R_0^2/\xi^2 \gg \varepsilon$. It follows from Eqs. (9) and (10), that the electron heating stops during the laser pulse if the pulse duration exceeds

$$\tau_{\max} \approx \frac{1}{\omega} \left(\frac{eE_0}{m_e \omega^2 R_0} \right)^{-2} \approx \frac{1}{\omega} \frac{R_0^2}{\xi^2}, \tag{11}$$

where ξ is defined by Eq. (6).

Until the electron heating slows down ($t < \tau_{\max}$), the amount of energy that the electrons absorb from the laser field is roughly εN_{ext} per laser period. Thus the power absorbed by a single cluster can be estimated as

$$P_c \approx \omega \varepsilon N_{ext} \approx E_0^2 R_0^3 \omega \frac{|e| E_0}{m_e \omega^2 R_0}. \tag{12}$$

Finally, once the electron energy reaches $\max \varepsilon_e$, the hot electrons begin to leak out.

Indeed, the charge of the cluster with all the hot electrons gone is estimated as $|e|N_H$. The corresponding binding energy for an electron is comparable to $\max \varepsilon_e$:

$$\frac{1}{2} m_e R_0^2 \omega^2 \approx \frac{e^2 N_H}{R_0}. \tag{13}$$

This means that, by the time the stochastic heating slows down, a significant fraction (about a half) of the hot electrons will escape from the cluster. The kinetic energy of the escaped electrons should be comparable to $\max \varepsilon_e$.

III. ION DYNAMICS

We have shown that the dynamics of the cluster electrons can vary, depending on the strength of the laser field and the cluster radius. There are three qualitatively different regimes with regard to the cluster size: small clusters ($R_0 < d_0$), medium clusters ($d_0 < R_0 < \xi$), and large clusters ($d_0 < \xi < R_0$). In what follows, we describe the ion dynamics for each case.

A. Small clusters ($R_0 < d_0$)

In this regime, all the electrons are extracted out of the cluster and they do not affect the dynamics of the ion explosion. The ions accelerate in the electric field of their own space-charge, with the ion energy after the explosion given by [13]

$$\varepsilon_i = \frac{1}{3} m_i \omega_{pi}^2 r_0^2, \tag{14}$$

where r_0 is the initial position of the ion in the cluster ($R_0 \geq r_0 \geq 0$) and $\omega_{pi} \equiv \sqrt{4\pi n_0 e^2/m_i}$. The time that it takes for the cluster to explode (double its radius) is roughly

$$\tau_i \approx 1/\omega_{pi}. \tag{15}$$

In this case, all the cluster ions are involved in the explosion. Typically, the explosion time is much longer than the laser period: $\tau_i \omega \gg 1$.

B. Medium clusters ($d_0 < R_0 < \xi$)

If the laser pulse is sufficiently short, so that the ions do not expand during the pulse, then after the pulse the cluster consists of a neutral core surrounded by a positive ion shell. The ion shell expands radially outwards on an ion time-scale. The ion kinetic energy after the expansion is given by [10]

$$\varepsilon_i = \frac{m_i \omega_{pi}^2 [r_0^3 - (R_0 - d_0)^3]}{3r_0}, \tag{16}$$

where r_0 is the initial position of the ion in the shell ($R_0 \geq r_0 \geq R_0 - d_0$). The number of ions involved in the explosion is given by Eq. (3). It follows from Eq. (16), that the characteristic ion energy is

$$\varepsilon_i \approx |e| E_0 R_0. \tag{17}$$

The duration of the explosion is roughly the time it takes for the ion shell to double its radius:

$$\tau_i \approx \sqrt{\frac{m_i R_0}{|e| E_0}}. \tag{18}$$

Therefore, the short laser pulse approximation holds if the pulse duration is much smaller than τ_i.

If the laser pulse is larger than τ_i, the ion expansion significantly affects the dynamics of the cold electron core. The ion expansion during the pulse can cause leakage of the cold electrons out of the cluster. In order to demonstrate this phenomenon, we simplify the picture assuming that the ions expand uniformly. As the cluster radius (R) increases from its initial value R_0, the plasma frequency decreases as $R^{-3/2}$ and, consequently, the core displacement increases as R^3 [see Eq. (2)]. Since the core displacement increases faster than the radius, the total number of the core electrons decreases in the expanding cluster. All the electrons, which were confined prior to expansion, escape from the cluster when the core displacement becomes equal to the instantaneous radius of the cluster R. This happens when $R = R_0\sqrt{R_0/d_0}$. After the electrons escape, the cluster explosion becomes similar to the explosion described in Subsection III A. Thus we can immediately find the characteristic

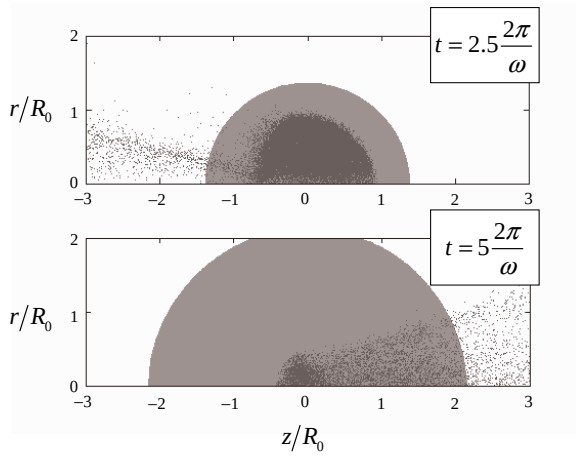

FIG. 4: Electron leakage due to the cluster expansion. The upper plot is a snapshot of the cluster configuration at $t = 2.5(2\pi/\omega)$, whereas the lower plot is a snapshot at $t = 5(2\pi/\omega)$, with electrons and ions shown as dark-grey and light-grey dots respectively.

ion energy after the explosion in terms of the initial parameters:

$$\varepsilon_i \approx |e|E_0 R_0 \sqrt{\frac{R_0 m_e \omega_{p0}^2}{|e|E_0}}. \tag{19}$$

This energy is higher than the ion energy in the case without electron leakage [see Eq. (17) for comparison].

In reality, the situation is more complex, because the ion expansion is not uniform and the expansion dynamics depends on the amplitude of the core oscillations, which can be enhanced [1] when the laser frequency meets the Mie resonance frequency [14]. Not all ions are exposed to the electrostatic field of the cluster, as ions deep inside the cluster can be temporarily shielded by the oscillating electron core. The duration of the laser pulse can also affect the number of the expanding ions. In order to be more quantitative, a self-consistent simulation of the ion and electron motion is required. We have developed an electrostatic particle-in-cell code [7, 16] that is capable of doing so with very modest computational requirements. An example of a self-consistent simulation for a medium-size cluster is shown in Fig. 4.

C. Large clusters ($d_0 < \xi < R_0$)

In this case, hot electrons accumulate in the cluster and they affect ion dynamics during the explosion. Since the electron heating occurs over many laser periods, the cluster may expand simultaneously during sufficiently long laser pulses.

We start with the regime when the laser pulse is so short that the ion shell expands only after the laser pulse. Then the number and the energy of the hot electrons depend on the duration of the laser pulse as discussed in Sec. II.

If the pulse duration exceeds τ_{max} given by Eq. (11), then electron heating stops already during the pulse. In this case, the total number of the hot electrons is given by Eq. (8) and their characteristic energy – by Eq. (10). This regime is somewhat similar to the case with $d_0 < R_0$ and $\xi \gg R_0$, because a noticeable part of the hot electrons escape. The effect of the remaining hot electrons on the ion dynamics is roughly the same as the effect of the ion space-charge. Therefore, we can estimate the ion energy assuming that all hot electrons are gone. It follows from Eq. (13) that the ion energy after the explosion is comparable to the energy of the hot electrons:

$$\varepsilon_i \approx \frac{1}{2} m_e R_0^2 \omega^2. \tag{20}$$

The total number of the accelerated ions is roughly equal to the total number of the hot electrons.

We now consider the case of a shorter laser pulse, such that $\tau \leq \tau_{laser} \leq \tau_{max}$, where τ_{laser} is the pulse duration and τ and τ_{max} are defined by Eqs. (7) and (11). After such pulse, the cluster consists of a neutral core, a thin positive ion shell, and a negative hot electron shell that is much thicker than the ion shell. The charge of the ion shell and the charge of the hot electron shell are roughly the same. The electric field that is created in the electron shell due to the charge separation is such that the corresponding drop in the electrostatic potential is equal to the characteristic electron energy, since this potential drop confines the hot electrons. If the energy of the hot electrons is much smaller than $\max \varepsilon_e$, then the electron and ion shells can be viewed as a narrow double layer at the very edge of the cluster.

Passing through the double layer, the ions from the ion shell gain energy comparable to the energy of the hot electrons. As a result of the acceleration, the ion density drops from n_0 to the density of the hot electrons, which is much smaller than n_0. After the ion shell

reaches the thickness of the electron shell, the hot electrons start to expand together with the ions (to satisfy the quasi-neutrality condition). As the electrons cool down via adiabatic expansion, their energy converts into the ion kinetic energy. The resulting energy gain is of the same order as the energy gain due to the ion acceleration in the double layer. After the initial ion shell expands, a new one is formed in its place, so that there is always a double layer at the edge of the cold electron core. A rigorous solution for the double layer and the resulting quasi-neutral plasma flow is given in Sec. V.

The double layer disappears when all hot electrons are gone from the cluster core. Therefore, the number of fast ions that the cluster produces during the explosion is determined by Eq. (8). This mechanism generates fast ions with energy

$$\varepsilon_i \approx m_e \frac{\tau_{laser}^2}{R_0^2} \left(\frac{eE_0}{m_e \omega} \right)^4 , \tag{21}$$

where τ_{laser} is the pulse duration.

In the case of a very short laser pulse with $\tau_{laser} \ll \tau$, where τ is defined by Eq. (7), the energy and the number of the fast ions are considerably lower than in the previous case. This regime is of little interest in the context of neutron production and we will skip it here.

As seen from Eq. (20), the energy of the ions resulting from the explosion of a large cluster can be as high as $m_e R_0^2 \omega^2/2$ if the laser pulse is sufficiently long. The ion energy increases with the cluster size until the cluster expansion begins to affect electron heating.

The rate of stochastic electron heating decreases significantly when the thickness of the hot outer shell becomes comparable to the initial cluster radius R_0. As shown in Sec. V, the shell expands with roughly the sound-speed $C_s \approx \sqrt{\varepsilon_e/m_i}$. Therefore, the electron heating time is limited by R_0/C_s. The corresponding electron energy follows directly from Eq. (9):

$$\varepsilon_e \approx m_e \sqrt{\frac{m_i}{m_e}} \left(\frac{eE_0}{m_e \omega} \right)^2 . \tag{22}$$

As a result of expansion, the hot electrons eventually cool down.

On the other hand, the electron heating stops even without expansion if the electron energy reaches $\max \varepsilon_e$, given by Eq. (10). Comparing Eqs. (10) and (22), we find the critical cluster radius:

$$R_* \approx \xi \left(\frac{m_i}{m_e} \right)^{1/4} . \tag{23}$$

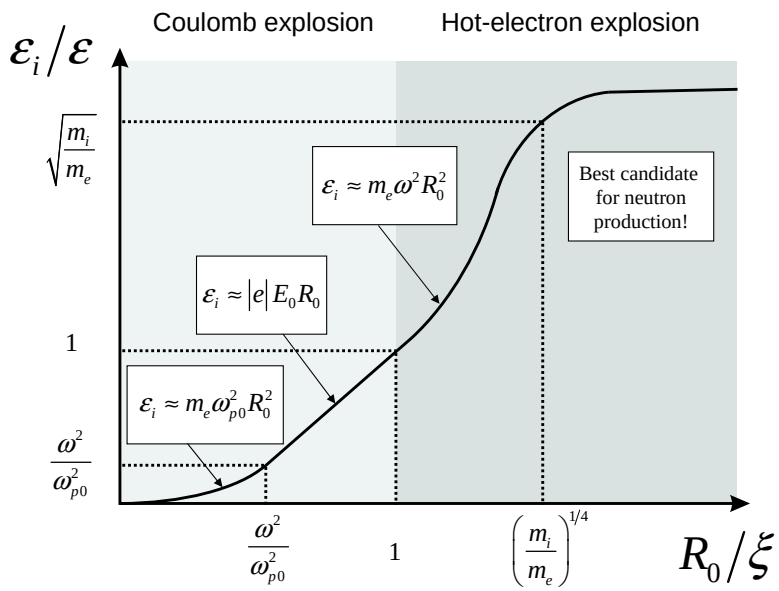

FIG. 5: Schematic plot of the ion energy as a function of cluster radius R_0 for a given laser field amplitude E_0. The cluster radius is normalized to ξ, which is the quivering amplitude of a free electron in the laser field E_0 [ξ is given by Eq. (6)]. The ion energy is normalized to the oscillation energy ε of a free electron in the laser field [ε is given by Eq. (4)].

For $R_0 < R_*$, the heating stops before the cluster expands and the characteristic ion energy scales as R_0^2 [see Eq. (10)]. For $R_0 > R_*$, the cluster expansion is significant and the ion energy is independent of the cluster radius [see Eq. (22)].

The results of this section are summarized in Fig. 5, which shows the ion energy as a function of the cluster radius for a given laser field amplitude E_0.

IV. ION ANISOTROPY

It has been observed that the ion spectrum is not isotropic in the laser-cluster experiments [15]. Moreover, the observed anisotropy depends on the laser field polarization.

There are two different origins of the ion spectrum anisotropy. First, the explosion of an individual cluster can be anisotropic. Second, after the explosion, the ions and electrons spread out to form a plasma filament. Any hot electrons that escape from the cluster are bound to the filament because of quasi-neutrality. The hot electron pressure forces the plasma to expand, further accelerating the ions. Since the filament is usually elongated in the direction of the laser pulse propagation, the ambipolar field is primarily radial, which can contribute to the anisotropy in the ion spectrum.

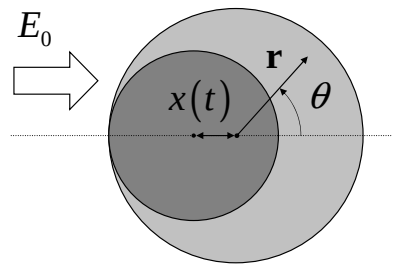

FIG. 6: Spherical cluster with an oscillating electron core.

In what follows, we discuss the single cluster anisotropy in more detail. The oscillating laser field does not directly affect the ion motion, since the time-averaged value of this field is virtually zero. However, the ion motion can be affected indirectly (by changing the electron space-charge inside the cluster or by changing the electron pressure).

If $d_0 > R_0$, then the cluster is fully stripped of electrons and the ion spectrum should depend solely on the initial shape of the cluster.

If $d_0 < R_0$ and $\xi \gg R_0$, then there is a cold electron core inside the cluster, which oscillates with the laser frequency. The core moves along the direction of the laser electric field and thus the electron space-charge, averaged over the laser period, is elongated in the same direction. As a result, the force acting on the ions during the expansion is not isotropic even for a spherical cluster.

In order to illustrate the elongation effect of the time averaged electron space-charge in the regime with $d_0 < R_0$ and $\xi \gg R_0$, we consider a uniform spherical cluster in a uniform linearly polarized field:

$$E(t) = E_0 \sin(\omega t), \tag{24}$$

where E_0 and ω are the field amplitude and frequency.

We use spherical coordinates (see Fig. 6) to find the radial and azimuthal components of the instantaneous electric field inside the cluster:

$$E_r(\mathbf{r}) = E_0 \sin(\omega t)\cos\theta + E_{\max}\frac{R_e}{R_0}\left(\frac{r}{R_e} - \alpha\frac{r - x(t)\cos\theta}{l}\right), \tag{25}$$

$$E_\theta(\mathbf{r}) = -E_0 \sin(\omega t)\sin\theta - E_{\max}\frac{R_e}{R_0}\frac{x(t)\sin\theta}{l}, \tag{26}$$

where $x(t) = -d_0 \sin(\omega t)$ is the core displacement, $E_{\max}$ is defined by Eq. (1), and quantities

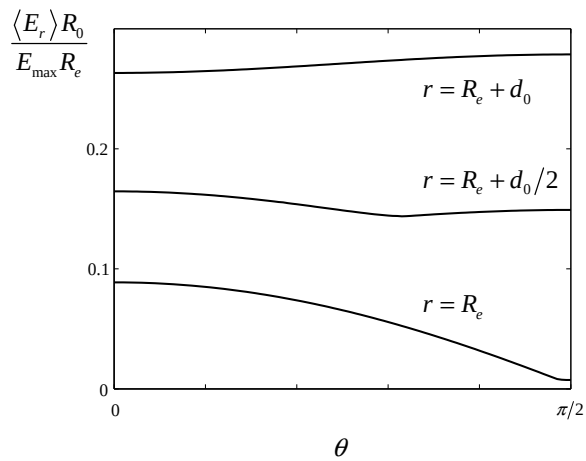

FIG. 7: Normalized radial component of the time-averaged electric field as a function of the azimuthal angle at different radii.

l and α are defined by:

$$l \equiv \sqrt{(r\sin\theta)^2 + (x(t) - r\cos\theta)^2}, \tag{27}$$

$$\alpha = l/R_e, \text{ for } l < R_e, \tag{28}$$

$$\alpha = R_e^2/l^2, \text{ for } l \geq R_e. \tag{29}$$

After averaging Eqs. (25) and (26) over the laser period, we find that

$$\langle E_r(\mathbf{r})\rangle = E_{\max}\frac{R_e}{R_0}\left[\frac{r}{R_e} - \left\langle \alpha \frac{r - x(t)\cos\theta}{l}\right\rangle\right], \tag{30}$$

$$\langle E_\theta(\mathbf{r})\rangle = -E_{\max}\frac{R_e}{R_0}\left\langle \frac{x(t)\sin\theta}{l}\right\rangle, \tag{31}$$

where the angular brackets stand for time averaging over the laser period.

For a relatively small displacement ($d_0/R_e \ll 1$), the electric field is primarily directed radially. The value of the electric field as a function of θ for $r = R_e$, $r = R_e + d_0/2$, and $r = R_e + d_0$ is shown in Fig. 7. The anisotropy is most pronounced for $r - R_e \ll d_0$, with the radial electric field much higher for $\theta = 0, \pi$ than for $\theta = \pm\pi/2$. It must be pointed out that the anisotropy changes its sign along the radius, becoming generally smaller at the cluster edge.

If $d_0 < R_0$ and $\xi \ll R_0$, then, in addition to the cold electron core, there are also hot electrons, which are bound to the cluster. Their pressure is likely to be anisotropic,

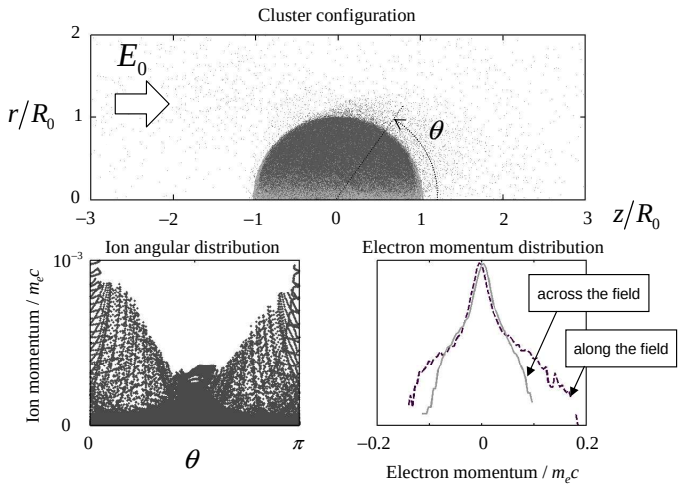

FIG. 8: Anisotropic ion expansion due to electron heating. The figures are snapshots of the cluster configuration and electron and ion distributions after 3 laser periods, for a cluster with the following parameters: $\xi/R_0 = 0.1$, $d_0/R_0 = 0.012$, and $\omega_{p0}/\omega = 5$. Each point on the ion distribution plot corresponds to an ion from the particle-in-cell simulation.

especially with a linearly polarized laser field. The pressure should be higher along the field axis, making the ion spectrum anisotropic in this case. Our particle-in-cell simulations [16] confirm this picture for clusters with $d_0 \ll \xi \ll R_0$. Figure 8 shows snapshots of the cluster configuration and electron and ion distributions after several laser periods. The anisotropic two-component electron distribution is well pronounced in this case. The ions gain larger momentum along the laser field, because of the anisotropic electron pressure.

V. ION ACCELERATION IN A LARGE CLUSTER

Expansion of a cluster with a cold electron core and hot electron halo deserves special attention because it exhibits interesting qualitative differences compared to the case of single-temperature electrons. In this section, we discuss a model problem that illustrates these differences. In accordance with the analysis of electron heating in Sec. II, we will imply that the density of the hot electrons is much smaller than the density of the cold electron core. It is then apparent that only the outer shell of the cluster ions will be involved in expansion since the cold electrons eliminate any electric field within the core, so that the ions within the core remain at rest. The problem of shell expansion is essentially one-dimensional as long as the shell thickness is much smaller than the cluster radius, which we herein assume to be the case. The main volume of the cluster provides virtually unlimited supply of ions, restricted

only by space-charge effects. In what follows, we will show that, under such circumstances, the solution for the ion flow in the shell consists of two matching parts: a steady state double layer adjacent to the core boundary and a quasi-neutral rarefaction wave at the leading edge of the expanding shell (see Fig. 9). The hot electrons in the shell are constantly renewed as every such electron travels across the entire cluster. In the thin shell limit, expansion of the shell hardly changes the total volume of the hot electron population. It is then allowable to neglect adiabatic cooling of the hot electrons during shell expansion. The main volume of the cluster serves as a large energy reservoir that maintains a constant energy distribution of the hot electrons. For the sake of simplicity, we will also neglect any power deposition from the laser during the expansion phase. To be specific, we will choose a Maxwell-Boltzman distribution of the hot electrons with a constant temperature T, although similar solutions can be found for other distribution functions. We thus have

$$n_e = n_{hot} \exp |e| \varphi / T, \tag{32}$$

where n_e is the local electron density of hot electrons and n_{hot} is their density in the core (we choose the electrostatic potential φ to be zero in the core). Next to the core, in the double layer with stationary ion flow, the ion density is

$$n_i = j / \sqrt{-2 |e| \varphi / m_i}, \tag{33}$$

where j =const is the ion flux (to be determined). Given Eqs. (32) and (33), the Poisson equation takes the form

$$\frac{d^2 \varphi}{dx^2} = -4\pi |e| \left[\frac{j}{\sqrt{-2 |e| \varphi / m_i}} - n_{hot} \exp |e| \varphi / T \right], \tag{34}$$

where the coordinate x is counted from the boundary of the cold core.

This equation has a well-known first integral,

$$\frac{1}{2} \left(\frac{d\varphi}{dx} \right)^2 = 4\pi |e| \left[\frac{\sqrt{2} j \sqrt{-\varphi}}{\sqrt{|e| / m_i}} + \frac{n_{hot} T}{|e|} \left(-1 + \exp |e| \varphi / T \right) \right], \tag{35}$$

where the integration constant is chosen to satisfy the condition that the electric field van-

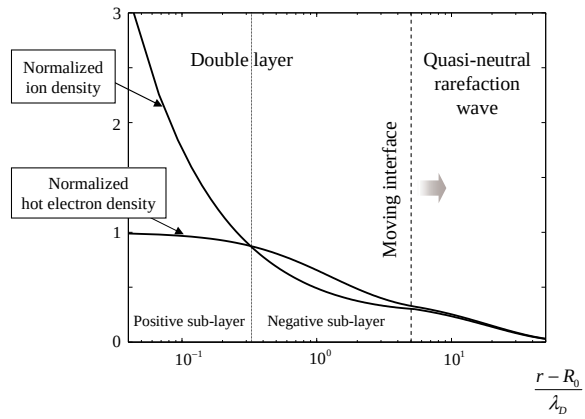

FIG. 9: Snapshot of the electron and ion density profiles in the expanding outer shell. The densities are normalized to the density of the hot electrons inside the cluster (n_{hot}). The log-scale is used for the normalized radial coordinate, $(r - R_0)/\lambda_D$, in order to show the narrow double layer adjacent to the cold electron core, where the normalization scale is defined as $\lambda_D \equiv \sqrt{T/4\pi n_{hot} e^2}$. The plots represent numerical solution of Eq. (35), matched to Eq. (42).

ished at the cold core boundary. The electric field should also be close to zero at the other side of the double layer, where the flow becomes quasi-neutral. Hence, the right-hand sides of Eqs. (34) and (35) must vanish simultaneously in the transition region from the steady state double layer to the quasi-neutral rarefaction wave. This requirement readily gives the ion flux and the value of the electrostatic potential at the (yet undetermined) transition point,

$$\varphi = -\frac{T}{|e|}\psi, \tag{36}$$

$$j = n_{hot}\sqrt{2\frac{T}{m_i}}\sqrt{\psi}\exp\left(-\psi\right). \tag{37}$$

In these expressions, $\psi \approx 1.257$ is the root of the algebraic equation $1 + 2\psi = \exp\psi$. The solution of Eq. (35) approaches the transitional potential (36) asymptotically at large values of x. Although this solution formally extends to arbitrarily large x, it fails to meet the condition that ion density vanishes at the leading edge of the expanding shell. In the presented steady-state flow, the asymptotic values (n_* and v_*) of the ion density and velocity are:

$$n_* = n_{hot}\exp(-\psi), \tag{38}$$

$$v_* = \sqrt{\frac{2T}{m_i}}\psi. \tag{39}$$

We now show that these values can be asymptotically matched at large x to a time-dependent flow that describes a quasi-neutral rarefaction wave with vanishing ion density at $x \to \infty$. The rarefaction wave is governed by the following set of fluid equations for the ion density n and velocity v:

$$\frac{\partial v}{\partial t} + v\frac{\partial v}{\partial x} = -\frac{T}{m_i}\frac{1}{n}\frac{\partial n}{\partial x}, \tag{40}$$

$$\frac{\partial n}{\partial t} + \frac{\partial}{\partial x} nv = 0. \tag{41}$$

It is straightforward to check that Eqs. (40) and (41) admit the following self-similar solution [17, 18]:

$$\ln\frac{n}{n_{**}} = -1 - \frac{1}{\sqrt{T/m_i}}\frac{x - x_{**}}{t - t_{**}}, \tag{42}$$

$$v = \sqrt{T/m_i} + \frac{x - x_{**}}{t - t_{**}}, \tag{43}$$

where n_{**}, x_{**}, and t_{**} are arbitrary constants. Let now x_* be a time-dependent matching point of the double layer and the rarefaction wave. By comparing Eqs. (42) and (43) with Eqs. (38) and (39), we then find that

$$\ln\frac{n_{hot}}{n_{**}} = \psi - \sqrt{2\psi}, \tag{44}$$

$$\frac{x_*(t) - x_{**}}{t - t_{**}} = \sqrt{T/m_i}\left(\sqrt{2\psi} - 1\right), \tag{45}$$

The values of the constants x_{**} and t_{**} depend on initial conditions in the shell and they can in principle be found with a more detailed analysis that includes a slight deviation from quasi-neutrality at the matching point. However, these constants are actually of little interest in the asymptotic regime since x and t eventually become much larger than x_{**} and t_{**}. It is important to point out that the ion flow is supersonic at the exit from the double layer, which ensures that the matching point moves away from the cluster edge, creating a continuously broadening spatial interval for the stationary flow. We thus observe that the rarefaction wave provides the needed transient solution that asymptotically allows a stationary ion flow in its wake. As noted by several authors [19, 20], the self-similar solution, given by Eqs. (42) and (43), needs to be corrected at the front edge of the rarefaction wave

where quasi-neutrality breaks down due to exponential decay of the ion density. This issue has been addressed in great detail in Ref. [19] that deals with a closely related problem of plasma expansion with isothermal electrons. The front-edge issue is a common element of our work and Ref. [19], so that the corresponding analysis of Ref. [19] is fully applicable to our case. The key difference between our problem and the one solved in Ref. [19] is the existence of a double layer at the cluster edge, as opposed to the positively charged layer found in Ref. [19]. The double layer that produces supersonic ions establishes exclusively due to the two-component structure of the electron distribution function, which is specific to cluster explosion.

VI. CONCLUDING REMARKS

A model of neutron production from exploding deuterium clusters was developed in Ref. [13]. Aimed at interpretation of present experiments with relatively small clusters [3, 4], this model involves an assumption that only bare-ion clusters contribute to neutron yield. For a given laser field, the model limits the radius of the participating clusters, so that larger clusters are excluded from consideration. On the other hand, neutron yield is known to be predominantly associated with the fastest ions that arise from the largest clusters. It would therefore be important to improve the model of Ref. [13] by including two additional ion production mechanisms that are specific to large clusters. The first one is Coulomb expansion of the ion shell, which occurs if the cluster radius is greater than the shell thickness (incomplete electron extraction), but still smaller than the free-electron excursion ξ in the laser field, so that all the extracted electrons leave the cluster and never come back. Within this window, the maximum energy of an accelerated ion increases roughly linearly with the cluster radius [see Eq. (17)], as opposed to the R_0^2 scaling for bare-ion clusters [see Eq. (14)]. The second mechanism is associated with stochastic heating of electrons that cross the cluster boundary, but still remain trapped electrostatically. As shown in Section II, the maximum energy of those electrons (for immobile ions) can be estimated as $m_e R_0^2 \omega^2/2$ [see Eq. (10)], provided that the laser pulse is sufficiently long. Remarkably, this energy is independent of the laser intensity as is the number of the stochastically heated electrons [see Eq. (8)]. Once heated, the hot electrons expand together with the equal number of ions (to satisfy the quasi-neutrality constraint). As the electrons cool down via adiabatic

expansion, their energy converts into the ion kinetic energy. This mechanism can produce fast ions with characteristic energy of order of $m_e\sqrt{\frac{m_i}{m_e}}\left(\frac{eE_0}{m_e\omega}\right)^2$ (see Fig. 5). A more detailed analysis shows that the ions gain significant part of their ultimate energy while they pass through a narrow double layer that forms at the very edge of the cluster where the ion density drops from the density of the cold core to roughly the density of the hot electrons. It is noteworthy that the underlying factor for this mechanism is a two-component electron distribution function in the cluster, which indicates the critical need for a kinetic description of the cluster electrons as opposed to hydrodynamic description with a single temperature that would not be appropriate for neutron yield calculation. A similar mechanism of ion acceleration in a hot Debye sheath was proposed in Ref. [21] as a qualitative explanation of hot ion production at the back surface of a thin planar target irradiated by a Petawatt laser. As inferred from numerical simulations [22], hot electron energy is of the order of ponderomotive potential in the plane target case, which is consistent with one-time vacuum heating. In clusters, multiple-pass stochastic vacuum heating allows the electrons to attain higher energies, giving rise to faster ions. An apparently high sensitivity of the neutron yield to the fast ion spectrum makes it generally difficult to quantitatively predict the yield for specific experimental parameters. However, it is quite conceivable that neutron measurements (together with additional diagnostics) can conclusively tell whether fast ions arise predominantly from the bare-ion cluster explosion or from the outer shell expansion under pressure of the hot electron population.

Our analysis in Section III indicates that experiments with large deuterium clusters (of about 50 nm in radius) would show a considerably higher neutron yield than that obtained in Ref. [3] from relatively small clusters of 2-5 nm. The main difficulty in conducting such high-yield experiments appears to be production of large clusters.

Acknowledgments

This work was supported by NSF FOCUS center and by the U.S. Department of Energy Contract No. DE-FG03-96ER-54346. We thank Dr. Todd Ditmire, Dr. Michael Downer, Dr. Charles Chiu, and Dr. Paul Parks for stimulating discussions.

[1] T. Ditmire, T. Donnely, A.M. Rubenchik, R.W. Falcone, M.D. Perry, Phys. Rev. A **53**, 3379 (1996).

[2] V.P.Krainov and M.B.Smirnov, Physics Reports **370**, 237 (2002).

[3] T. Ditmire, J. Zweiback, V.P. Yanovsky, T.E. Cowan, G. Hays, and K.B. Wharton, Nature **398**, 489 (1999).

[4] J. Zweiback, R.A. Smith, T.E. Cowan, G. Hays, K.B. Wharton, V.P. Yanovsky, and T.Ditmire, Phys. Rev. Lett. **84**, 2634 (2000).

[5] T.Ditmire, Contemporary Physics **38**, 315 (1997).

[6] B.Shim, G.Hays, M.Downer, and T.Ditmire, Bull. Am. Phys. Soc. **48**, 24 (2003).

[7] M.V.Fomyts'kyi, B.N.Breizman, A.V.Arefiev, and C.Chiu, Phys. Plasmas **11**, 3349 (2004).

[8] S.Fomichev, S.Popruzhenko, D.Zaretsky, and W.Becker, Jornal of Physics B **36**, 3817 (2003).

[9] S.Fomichev, S.Popruzhenko, D.Zaretsky, and W.Becker, Optical Express **11**, 2433 (2003).

[10] B.N.Breizman and A.V.Arefiev, Plasma Physics Reports **29**, 593 (2003).

[11] F.Brunel, Phys. Rev. Lett. **59**, 52 (1987).

[12] F.Brunel, Phys. Fluids. **31**, 2714 (1988).

[13] P.B.Parks, T.E.Cowan, R.B.Stephens, and E.M.Campbell, Phys. Rev. A **63**, 063203 (2001).

[14] G.Mie, Ann. Physik **25**, 377 (1908).

[15] Private comunications with Dr. Kirk Madison (2002).

[16] M.V.Fomyts'kyi, Ph.D. Thesis, University of Texas at Austin, 2004.

[17] A. V. Gurevich, L. V. Pariiskaya, and L. P. Pitaevskii, Sov. Phys. JETP **22**, 449 (1966).

[18] L.D.Landau and E.M.Lifshitz, *Course of Theoretical Physics, Vol. 6, Fluid Mechanics* (Pergamon Press, London, 1959).

[19] P.Mora, Phys. Rev. Lett. **90**, 185002 (2003).

[20] A. V. Gurevich and A. P. Meshcherkin, Zh. Eksp. Teor. Fiz. **53**, 1810 (1981) [Sov. Phys. JETP 53, 937 (1981)].

[21] S. P. Hatchett, C. G. Brown, T. E. Cowan, E. A. Henry, J. S. Johnson, M. H. Key, J. A. Koch, A. B. Langdon, B. F. Lasinski, R. W. Lee, A. J. Mackinnon, D. M. Pennington, M. D. Perry, T. W. Phillips, M. Roth, T. C. Sangster, M. S. Singh, R. A. Snavely, M. A. Stoyer, S. C. Wilks, and K. Yasuike, Phys. Plasmas **7**, 2076 (2000).

[22] B. F. Lasinski, A. B. Langdon, S. P. Hatchett, M. H. Key, and M. Tabak, Phys. Plasmas **6**, 2041 (1999).